JCTC Journal of Chemical Theory and Computation

Article

pubs.acs.org/JCTC

Critical Evaluation of Implicit Solvent Models for Predicting Aqueous Oxidation Potentials of Neutral Organic Compounds

Jennifer J. Guerard and J. Samuel Arey*

Environmental Chemistry Modeling Laboratory, Swiss Federal Institute of Technology at Lausanne (EPFL), GR C2 544, Station 2, 1015 Lausanne, Vaud, Switzerland

Swiss Federal Institute of Aquatic Science and Technology (Eawag) Überlandstrasse 113, 8600 Dübendorf, Zurich, Switzerland

Supporting Information

ABSTRACT: Quantum chemical implicit solvent models are used widely to estimate aqueous redox potentials. We compared the accuracy of several popular implicit solvent models (SM8, SMD, C-PCM, IEF-PCM, and COSMO-RS) for the prediction of aqueous single electron oxidation potentials of a diverse test set of neutral organic compounds for which accurate experimental oxidation potential and gas-phase ionization energy data are available. Using a thermodynamic cycle, we decomposed the free energy of oxidation into contributions arising from the gas-phase adiabatic ionization energy, the solvation free energy of the closed-shell neutral species, and the solvation free energy of the radical cation species. For aqueous oxidation potentials, implicit solvent models exhibited mean unsigned errors (MUEs) ranging from 0.27 to 0.50 V, depending on the model. The principal source of error was attributed to the computed solvation free energy of the oxidized radical cation. Based on these results, a recommended implicit solvation approach is the SMD model for the solvation free energy combined with CBS-QB3 for the gas-phase ionization energy. With this approach, the MUE in computed oxidation potentials was 0.27 V, and the MUE in solvation free energy of the charged open-shell species was 0.32 eV. This baseline assessment provides a compiled benchmark test set of vetted experimental data that may be used to judge newly developed solvation models for their ability to produce improved predictions for aqueous oxidation potentials and related properties.

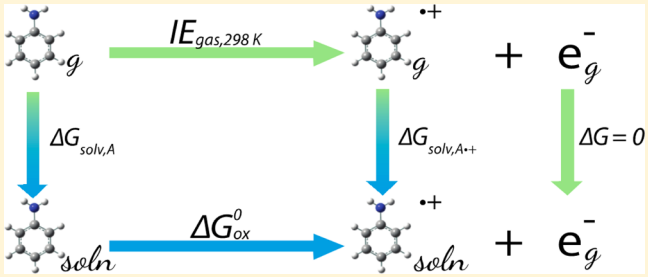

1. INTRODUCTION

One-electron oxidation processes are widely relevant for the transformations of organic compounds in aquatic, aerosol, and biological systems. For example, in aquatic systems, photochemically excited dissolved organic matter can oxidize natural water constituents and anthropogenic contaminants including phenylureas,[1] sulfonamides,[2] and substituted phenols.[3] In biological systems, single electron transfer (SET) is an essential reaction step for several biochemical pathways. SET serves as the first step in photosynthesis,[4] plays a role in DNA damage and repair,[5] and may also be important in understanding the reactivity of pharmacologically active substances.[6] Additionally, some biologically active molecules have antioxidant properties that control oxidative stress within biological systems. Examples include quinones,[7] anilines,[8] organophosphorous compounds,[9] glutathione,[10] and nucleic acid bases.[11]

The experimentally measurable oxidation potential indicates the free energy of electron transfer relative to a reference electrode, and therefore this property determines the feasibility of an oxidation reaction in a given context. Experimental techniques for measuring oxidation potentials can be categorized as equilibrium or nonequilibrium methods. Voltammetry, an equilibrium method, can only measure oxidation potentials when the electron transfer is reversible,[12] and this is often difficult to ensure in aqueous solution. Radical species resulting from such an electron transfer are often too short-lived in water to conduct a reliable reversible measurement using an electrochemical method.[12] Alternatively, nonequilibrium methods such as pulse radiolysis allow more accurate redox potential determinations for organic compounds in aqueous solution.[12−20] However, these challenging measurements are relatively few, and thus there are not many reported aqueous single-electron oxidation potentials for organic molecules by nonequilibrium methods. For example, due to the existence of multiple relevant acid−base equilibria for both oxidized and reduced species of nucleobases, accurate experimental aqueous redox potential measurements are not available for some nucleosides and related derivative structures.[11]

Quantum chemistry methods offer the possibility to estimate needed oxidation potentials that may be otherwise difficult to obtain. Two major classes of implicit solvent models have been developed that embed the solute in a specified cavity: continuum models and conductor-like screening models.[21] Continuum models use a parametrized dielectric medium

Received: May 29, 2013
Published: October 17, 2013

   dx.doi.org/10.1021/ct4004433 | J. Chem. Theory Comput. 2013, 9, 5046−5058

surrounding the solute cavity to represent the solvent polarization caused by charge separation of the solute.[21] An iterative approach is used to calculate the screening of the solute's electrostatic field by the continuum.[22] Examples of such models include polarizable continuum models (PCMs) such as IEF-PCM,[23−25] C-PCM,[26−28] and the SMx and SMD models.[29−31] In contrast, conductor-like screening models treat the solvent as a conductor of infinite permittivity, scaled by a factor that relates it to the dielectric constant of the desired solvent.[22] These models include COSMO[26] and COSMO-RS.[32,33] COSMO-RS, the "conductor-like screening model for real solvents", starts with a COSMO result and then treats the screening charge densities on contact segments on the surface of the solute cavity with a statistical thermodynamics framework. C-PCM is also a conductor-like model, but it is implemented within the PCM approach. These implicit solvent models have become widely used for understanding properties dependent on the free energy of solvation, such as aqueous oxidation potential,[4,5,8,11,34] aqueous reduction potential,[34−43] oxidation/reduction potentials in nonaqueous solvents,[44−51] aqueous pK_a,[52−57] and nonaqueous solvent pK_a.[58−60]

Relatively limited work has been done to assess and compare the performances of these implicit solvent models for the computation of aqueous oxidation potentials of diverse organic compounds; this contrasts with extensive comparative assessments of implicit models for solvation energies involving closed shell species. Winget et al. compared two different versions of SMx models for the computation of aqueous oxidation potentials of substituted anilines.[8] Bylaska et al. compared their COSMO results to SM5.42 data reported by Cwiertny et al. for computed aqueous one-electron reduction potentials of thirteen chlorinated aliphatic compounds, and they also compared computed results to experimental data for eleven other chlorinated aliphatics.[41,43] Zubatyuk et al.[36] investigated performance of I-PCM vs IEF-PCM for the computed reduction potentials of substituted nitrobenzenes in water. Sviatenko et al.[42] later compared IEF-PCM and C-PCM models with SMD for determining the aqueous reduction potentials of substituted nitrobenzenes. Hodgson et al.[34] evaluated the performance of IEF-PCM vs C-PCM for computing aqueous oxidation and reduction potentials of several substituted nitroxide radical structures. Because the nitroxide radical structures they investigated have relatively long lifetimes in aqueous solution, equilibrium experimental redox potential measurements were considered reliable in this particular case. Some of these and other studies have also assessed the influence of electronic structure method on the performance of implicit solvent models for aqueous redox potential computations.[11,34,36,42] Altogether, we found studies that looked into performances of implicit models for predicting aqueous potentials for reductive dehalogenation reactions,[4,37,41,43] oxidation of phenols and anilines,[4,8] reduction of quinones,[4,38−40] reduction of nitro-containing organics,[36,41,42] oxidation and reduction of nitroxide radicals,[34] and reduction and oxidation of nucleic acid structures.[5,11] While several of these studies compare computations against vetted experimental data sources, others could be questioned, reportedly comparing computed aqueous redox potentials to experimental values obtained in nonaqueous solvent, using data obtained from unreliable experimental sources, or failing to give citations for experimental data altogether. Based on this review, popular implicit solvent models have not been extensively assessed and compared for their ability to handle one-electron oxidations of a diverse set of neutral organic compounds in aqueous solution, using vetted experimental data.

In contrast to the situation for redox potentials, there exist assessments that have extensively assessed and compared implicit solvent models for predicting solvation free energies of diverse closed-shell neutral organic compounds and monovalent cations and anions.[31,61−70] Cramer and Truhlar compared the accuracies of several implicit solvent models (SM8, IEF-PCM, C-PCM, PBSA,[71,72] COSMO as implemented in NWChem[73,74]), evaluating them for solvation energies of a large database of diverse neutral, anionic, and cationic species in both aqueous and nonaqueous solvents.[61] Ho and Coote assessed several solvent models (SM6,[29] COSMO-RS, I-PCM,[75] C-PCM) for the calculation of aqueous pK_a values of a diverse test set of 55 organic and inorganic acids.[70] These studies followed the strategy employed in the early work of Liptak and Shields, in which a thermodynamic cycle was used to separate the gas-phase and solution phase contributions to proton dissociation of several carboxylic acids, enabling an evaluation of C-PCM for the prediction of pK_a values of those compounds.[53]

Implicit solvent models have been observed to exhibit systematic errors for redox potentials when applied within a given compound class.[4,8,40,65] For example, for a set of substituted anilines, Winget et al. attributed errors in computed oxidation potentials to deficiencies in the computed free energy of solvation of the radical cation species, reporting that they were consistently underestimated by 0.6 eV.[8] In order to accommodate these systematic biases, some groups propose to fit calculated potentials to experimentally measured data via linear regression. This method appears to produce improved estimates of oxidation potential values within a specific compound family. However, for many relevant organic compound families, oxidation potential data simply are not available in order to perform such fits. Other strategies have included redefining the solvent cavity or its size, as done by Yu et al. for pK_a values of aniline radicals in DMSO,[60] Zubatyuk et al. for the reduction potential of nitrobenzenes,[36] Sviatenko et al. for several different organic molecules in aqueous or nonaqueous solvent,[42] and by both Psciuk et al. and Paukku and Hill for oxidation potentials of nucleic acid bases.[5,11]

In this work, we sought to assess and compare currently popular continuum models for their ability to compute aqueous single electron oxidation potentials of a diverse set of neutral organic compounds. We evaluated these methods using carefully vetted experimental data. We compiled a database of high-accuracy experimental gas-phase ionization energies and one-electron oxidation potentials, measured in aqueous solution or acetonitrile, for a diverse set of simple organic compounds that represent common redox-active substructures of biomolecules, pharmaceuticals, environmental contaminants, and natural organic matter. We then evaluated several widely used implicit solvent models for their ability to predict accurate oxidation potentials for these compounds. From these data, we apportioned the errors arising from the modeled free energies of solvation of the neutral species and radical cation species, based on computed and experimental oxidation potentials in condensed phase and adiabatic ionization energies in the gas phase. To our knowledge, this is the first study to evaluate these implicit models side-by-side for their ability to predict oxidation potentials for a carefully vetted experimental data set involving diverse organic compounds.

Finally, we note that several studies have proposed the inclusion of explicit waters together with implicit solvent model calculations, in so-called "cluster-continuum" approaches, to improve predictions of pK_a values of small acids and solvation free energies of small closed-shell ions.[29,70,76,77] Hence, one may reasonably ask whether similar approaches should also be applied for redox potential calculations, and this is discussed briefly at the end of the article.

2. COMPUTATIONAL METHODS

The loss of an electron in aqueous phase is defined as:

$$A_{soln} \rightarrow e^-_g + A^{\bullet+}_{soln} \quad (1)$$

However, from a computational standpoint it is convenient to use a thermodynamic cycle (Figure 1) and separate the free

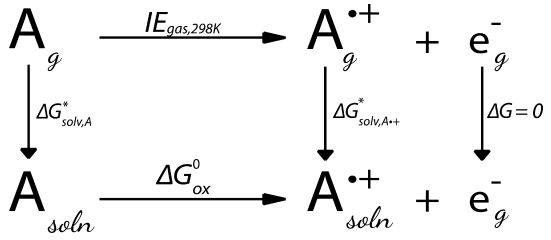

Figure 1. Thermodynamic cycle. IE_{gas} is the gas-phase ionization energy at 298 K. ΔG^0_{ox} is the aqueous free energy of oxidation at 298 K. $\Delta G^*_{solv,A}$ is the free energy of solvation of the (reduced) neutral closed shell species; $\Delta G^*_{solv,A\bullet+}$ is the free energy of solvation of the (oxidized) radical open shell species, both at 298 K. The lone electron, e^-, is at 298 K, consistent with the electron convention.

energy of reaction, ΔG^0_{ox}, into the sum of the gas-phase adiabatic ionization energy (IE_{gas}) and the difference in free energy of solvation between the oxidized and reduced species, $\Delta\Delta G_{solv}$,

$$\Delta G^0_{ox} = IE_{gas}(298\ \mathrm{K}) + \Delta\Delta G_{solv} \quad (2)$$

$$\Delta\Delta G_{solv} = \Delta G^*_{solv,A\bullet+} - \Delta G^*_{solv,A} \quad (3)$$

where $\Delta G^*_{solv,A}$ is the free energy of solvation of the reduced closed shell neutral species, and $\Delta G^*_{solv,A\bullet+}$ is the free energy of solvation of the oxidized open shell cation species. The free energy of reaction, ΔG^0_{ox}, is notated with the standard state of 1 atm in the gas phase and 1 mol/L in the solution phase. However, implicit solvent model computations normally employ a standard state of 1 mol/L in the gas phase and 1 mol/L in the aqueous phase, denoted by the superscript *, which is the convention also used for reporting the experimental free energies of solvation in the present work. Hence, to compute ΔG^0_{ox}, one would need to add 1.89 kcal/mol to the solvation free energy of each molecular species, which is the free energy associated with compressing an ideal gas (1 atm) to its density in the aqueous standard state (1 mol/L). However, the number of molecular species does not change during the oxidation half-reaction in eq 1 and the lone electron is represented in the gas phase, hence the reference state correction cancels out in eq 3, allowing us to compute ΔG^0_{ox} using eq 2. The resulting free energy of oxidation, ΔG^0_{ox}, can then be used to determine the oxidation potential,

$$E_{ox} = -\left(\frac{-\Delta G^0_{ox}}{\eta F} + \mathrm{SHE}\right) \quad (4)$$

where n is the number of electrons, F is the Faraday constant (96,485.3365 C/mol),[78] and SHE is the potential of the standard hydrogen electrode, 4.28 V.[79] Calculated ΔG^0_{ox} values were obtained using eqs 2 and 3, based on computations of IE_{gas}, $\Delta G^*_{solv,A}$, and $\Delta G^*_{solv,A\bullet+}$ as described below.

Gas-phase adiabatic ionization energies, IE_{gas}, were computed at both 0 and 298 K. We report computed IE_{gas} results at 0 K for the purposes of direct comparison to reported experimental IE_{gas} data measured using threshold ionization techniques (see section 3). We additionally computed IE_{gas} values at 298 K for the use with oxidation potential calculations via eqs 2−4. The oxidation potential data use the electron convention, which differs from the thermochemical convention used for the reported IE_{gas} data at 0 K (ion convention), in order to account for the enthalpy of formation of the electron at 298 K. Thus, IE_{gas} (298 K) values were obtained by adding together IE_{gas} (0 K), the thermal free energy of the molecular species at 298 K, and the integrated heat capacity of the electron at 298 K using Fermi-Dirac statistics (0.752 kcal/mol).[80]

All gas-phase geometries were optimized using M06-2X[81]/6-31G(d),[82,83] except where indicated otherwise, with the Gaussian 09 (v. B01) software package.[84] Stationary structures were confirmed using frequency analysis at the same level of theory. Electronic contributions to the gas-phase ionization energies were calculated in Gaussian 09 using the following protocols: CBS-QB3,[85,86] B2PLYP-D[87,88]/aug-cc-PVTZ,[89] M06-2X/6-31G(d), and M06-2X/aug-cc-PVTZ. CBS-QB3 energies were computed both with the default geometry optimization (B3LYP[90]/6-311G(2d,d,p)) and with geometries optimized from M06-2X/6-31G(d). However we found no significant differences in CBS-QB3 results with these two geometries, hence only the default CBS-QB3 calculations are reported here. ROCBS-QB3[91] calculations were additionally conducted for cases where at least one electronic structure method contribution to the composite CBS-QB3 energy was found to be spin contaminated with the $<S^2>$ value larger than 0.80. Thermal contributions to the free energy were computed using M06-2X/6-31G(d) for all gas-phase calculations, using the rigid rotor and harmonic oscillator approximations,[92] except for the CBS-QB3 method where the default B3LYP/6-311G(2d,d,p) thermal free energy was applied. These methods were considered adequate to capture thermal contributions to the free energy for the accuracy needed here.[93]

When employing implicit solvent models to compute free energies of solvation of both the neutral and radical species, we applied the default settings of the models, as we expect that most users will apply the methods in this way. Implicit solvent model calculations were conducted with the Gaussian 09 (for SMD, IEF-PCM, and C-PCM), Q-Chem (for SM8 calculations),[94] and ADF (for COSMO-RS)[95−97] software packages. Free energies of solvation were computed for both oxidized and reduced species using the M06-2X/6-31G(d) gas-phase optimized geometries with SMD,[31] SM8,[30] C-PCM,[26−28] IEF-PCM,[23−25] and COSMO-RS[26,32,33] for both aqueous solvent and in acetonitrile solvent. For all implicit solvent models that we evaluated, electronic structure was represented using a M06-2X/6-31G(d) single point calculation, except for COSMO-RS, where BP86[98,99]/cc-pVTZ was used. This exception was made because COSMO-RS calculations are not technically enabled

Table 1. Experimental and Computed Gas-Phase Adiabatic Ionization Energies (IE_{gas}) at 0 K (eV), Experimental Oxidation Potentials (E^0_{ox}) vs SHE (V) at 298 K, Experimental Change in Free Energy of Solvation upon Ionization ($\Delta\Delta G_{solv}$) at 298 K (eV), and Experimental in Free Energy of Solvation (ΔG^*_{solv}) at 298 K (eV)[e]

compound	$IE_{gas,\ expt\ (0\ K)}$[a]	$IE_{gas,\ (0\ K)\ CBS\text{-}QB3}$	$IE_{gas,\ (0\ K)\ ROCBS\text{-}QB3}$	$E^0_{ox,aq}$[b]	$E^0_{ox,ACN}$[c]	$\Delta\Delta G_{solv,aq}$	$\Delta G^*_{solv,aq,A}$[d]	$\Delta G^*_{solv,aq,A\bullet+}$	$\Delta\Delta G_{solv,ACN}$
phenol	8.5082 ± 0.0006	8.56		1.50		−2.79	−0.27	−3.06	
4-chlorophenol	8.4436 ± 0.0006	8.49	8.49	1.44		−2.75	−0.27	−3.02	
4-cyanophenol	9.0134 ± 0.0006	9.03	9.07	1.71		−3.08	−0.31	−3.39	
4-methoxyphenol	7.7129 ± 0.0025	7.78		1.23		−2.26	−0.34	−2.61	
4-methylphenol	8.1726 ± 0.0006	8.24		1.38		−2.58	−0.27	−2.85	
3,4-dimethoxyphenol		7.34		1.17		−1.96			
2,4,6-trimethylphenol		7.89		1.22	1.44	−2.45	−0.23	−2.68	−2.23
anisole	8.2322 ± 0.0006	8.28	8.30	1.62	1.99	−2.39	−0.10	−2.49	−2.02
1,2-dimethoxybenzene	7.6393 ± 0.0006	7.70		1.33	1.69	−2.09	−0.18	−2.27	−1.74
1,3-dimethoxybenzene	7.8756 ± 0.0006	8.09		1.55	1.75	−2.10	−0.14	−2.24	−1.90
1,4-dimethoxybenzene	7.5087 ± 0.0006	7.57		1.30	1.54	−1.99	−0.19	−2.18	−1.75
1,2,4-trimethoxybenzene		7.27		1.13	1.37	−1.93			−1.69
aniline	7.7204 ± 0.0006	7.73	7.75	1.02	1.17	−2.48	−0.24	−2.72	−2.33
4-toluidine	7.4587 ± 0.0006	7.47	7.49	0.92	1.02	−2.32	−0.21	−2.53	−2.22
N-methylaniline	7.4142 ± 0.0006	7.42	7.43	0.95	1.05	−2.24	−0.20	−2.44	−2.14
N,*N*′-dimethylaniline	7.1931 ± 0.0006	7.20	7.17		1.00		−0.15		−1.97
4-phenylenediamine	6.7723 ± 0.0006	6.79		0.59	0.73	−1.99	−0.36	−2.34	−1.85
indole	7.7604 ± 0.0005	7.82	7.79	1.24	1.45	−2.30	−0.27	−2.57	−2.09
1-methylindole	7.5317 ± 0.0006	7.60	7.57	1.23	1.44	−2.08	−0.18	−2.26	−1.87
2-methylindole		7.56	7.53	1.10	1.31	−2.20	−0.24	−2.44	−1.99
piperidine		8.04			1.54		−0.22		−2.28
DABCO	7.1950 ± 0.00003	7.01			0.80		−0.29		−2.19
N-butylamine		8.70			1.63		−0.20		−2.85
triethylamine		7.46			1.19		−0.14		−2.04
dimethylsulfide	8.6903 ± 0.0009	8.69		1.66		−2.79	−0.07	−2.86	
dimethyldisulfide		8.11		1.39		−2.49	−0.08	−2.56	
thioanisole		7.95	7.93	1.45	1.58	−2.28	−0.13	−2.41	−2.15

[a]References 103−117 and 135. [b]References 3, 13−15, 19, 136, and 137. [c]References 138−143. [d]Reference 101. [e]$IE_{gas,expt}$ refers to the experimental adiabatic gas-phase ionization energy. $IE_{gas,CBS\text{-}QB3}$ and $IE_{gas,ROCBS\text{-}QB3}$ refer to the adiabatic gas-phase ionization energy computed using CBS-QB3 and ROCBS-QB3, respectively. For experimental ionization energies, reported uncertainties are listed. Both experimental and computed gas-phase ionization energies are consistent with the ion convention at 0 K. Reported experimental and computed oxidation potentials are consistent with the electron convention at 298 K. Uncertainties in experimental aqueous oxidation potentials, $E^0_{ox,aq}$, are reported as ±0.02 V. Uncertainties in experimental acetonitrile oxidation potentials were not reported. $\Delta\Delta G_{solv,aq}$ refers to the difference in aqueous solvation free energy between the oxidized and reduced state of the molecule; $\Delta\Delta G_{solv,aq}$ was determined according to eq 6 based on reported experimental ionization energy and oxidation potential data. $\Delta\Delta G_{solv,ACN}$ refers to the difference in solvation free energy between the oxidized and reduced state in acetonitrile solvent, also determined using eq 6. $\Delta G^*_{solv,aq,\ A}$ is the aqueous solvation free energy of the neutral species, based on experimental data.[101] $\Delta G^*_{solv,aq,\ A\bullet+}$ is the aqueous solvation free energy of the oxidized radical species, estimated from experimental data according to eq 7.

for electronic structure methods other than BP86. Because implicit solvent model free energies are not found to be highly sensitive to basis set,[31] we did not extensively test basis set choices. Nonetheless, for aqueous phase solvation free energies, we additionally evaluated SM8/B3LYP/6-31G(d) and SMD/M06-2X/aug-cc-pVTZ. These results were used to briefly evaluate our supposition that implicit solvent model results were not highly sensitive to the choice of model chemistry and basis set, for the systems studied here, as long as the system electronic density is correct.

3. EXPERIMENTAL DATA

We evaluated a test set consisting of twenty-seven small aromatic and aliphatic organic molecules with diverse functional groups for which experimental oxidation potential data are available from pulse radiolysis (for aqueous solution data) or cyclic voltammetry (for acetonitrile solution data). The test set included substituted phenols, methoxybenzenes, substituted anilines, indoles, aliphatic amines, and organosulfur compounds (Table 1). For several of the selected compounds, high-quality experimental gas-phase adiabatic ionization energy data are also available, discussed further below. Reported oxidation potentials span a range from 0.59 to 1.71 V in water and 0.73 to 1.99 V in acetonitrile solution.

Discrepancies exist among reported experimental oxidation potential data from different sources, and a brief discussion about data quality is warranted. Data from pulse radiolysis methods were assigned an uncertainty of ±0.02 V.[13−15,19,20] Experimental oxidation potential data for the phenols in our test set were determined by Canonica et al. based on pK_a and pulse radiolysis measurements.[3] In an earlier study, Suatoni et al. also reported aqueous oxidation potential values for several phenols based on cyclic voltammetry data.[100] For the three phenols that are common to both studies (phenol, 4-methylphenol, 4-methoxyphenol), the reported oxidation potential values differ by over 0.5 V between cyclic voltammetry and pulse radiolysis measurements, once appropriate adjustments for the reference electrode are taken into account. The voltammetry data rely upon the assumption that the oxidation reaction is a reversible process; however, due to the short-lived nature of cation radicals in aqueous solution, it is unlikely that the equilibrium assumption is appropriate.[12] We considered

dx.doi.org/10.1021/ct4004433 | J. Chem. Theory Comput. 2013, 9, 5046−5058

pulse radiolysis data to be more reliable, and our selected aqueous oxidation potential data are taken exclusively from reported pulse radiolysis measurements. By contrast, in their evaluation of implicit solvent models for computing oxidation potentials, Winget et al. rely upon Suatoni et al. cyclic voltammetry data from experimental aqueous oxidation potential values of twenty-four phenols and twenty-two anilines.[4,8] Based on the questionable appropriateness of the cyclic voltammetry data for aqueous single-electron oxidation potentials, we think the results of the Winget et al. studies may need to be revisited. For oxidation potentials in acetonitrile solution, we did rely on reported voltammetry data, although most such reports did not list uncertainties.

For the case of 4-chlorophenol, the experimental oxidation potential was determined using the same approach as that of Canonica et al. for other phenols,[3] based on the reduction potential of the phenoxy radical species (0.80 ± 0.02 V)[20] and the experimental pK_a values of the neutral species (9.41)[101] and cation radical (−1.30):[102]

$$E_{ox}(PhOH/PhOH^{\bullet+}) = E_{ox}(PhO^{-}/PhO^{\bullet}) + 2.303RT[\mathrm{p}K_a(PhOH) - \mathrm{p}K_a(PhOH^{\bullet+})]/F \quad (5)$$

Using eq 5, the experimental aqueous oxidation potential for 4-chlorophenol was determined to be 1.44 V vs SHE.

Experimental gas-phase adiabatic ionization energies at 0 K had reported uncertainties that ranged from 0.00003 to 0.0025 eV, based on reported values determined by ZEKE (zero electron kinetic energy) or MATI (mass analyzed threshold ionization) methods.[103−117] These data are significantly more accurate than many listed entries in popular data compilations, which rely on mixed data sources of varied quality.[118,119]

Using the method outlined by Sviatenko et al.,[42] we calculated experimental $\Delta\Delta G_{solv}$ values from experimental aqueous oxidation potentials and experimental ionization energies, as described below. In cases where high-accuracy experimental ionization energies were not available, we used CBS-QB3 or ROCBS-QB3 ionization energies instead. By rearranging eqs 2−4, the change in free energy of solvation upon oxidation, $\Delta\Delta G_{solv}$, can simply be calculated from values of E^0_{ox}, SHE, and IE_{gas}:

$$\Delta\Delta G_{solv} = nF(E^0_{ox} + \mathrm{SHE}) - IE_{gas,298\ \mathrm{K}} \quad (6)$$

To be consistent with the electron convention and temperature of reported E^0_{ox} data (298 K), IE_{gas} values reported at 0 K were converted to 298 K by the inclusion of computed gas-phase thermal free energy values for the solute (computed using M06-2X/6-31G(d)) and the integrated heat capacity of the electron (0.752 kcal/mol).[80]

$\Delta\Delta G_{solv}$ represents the difference between the free energy of solvation of the oxidized radical species and the free energy of solvation of the reduced closed-shell species at 298 K (eq 3). Hence, using the values of $\Delta\Delta G_{solv}$ and $\Delta G^*_{solv,A}$, both of which were obtained from experimental data, we could determine the experimental solvation free energy of the oxidized radical species, $\Delta G^*_{solv,A\bullet+}$, in aqueous solution at 298 K:

$$\Delta G^*_{solv,A^{\bullet+}} = \Delta\Delta G_{solv} - \Delta G^*_{solv,A} \quad (7)$$

$\Delta G^*_{solv,A}$ data were determined from compilations of vapor pressure and aqueous solubility data[101] using the methods outlined in the MNSol database.[120] These data are listed in Table 1. Experimental aqueous $\Delta\Delta G_{solv}$ values were determined from experimental aqueous oxidation potentials and IE_{gas} data, using eq 6. For twenty of the twenty-seven compounds in this test set, sufficient experimental data were available to determine aqueous $\Delta G^*_{solv,A\bullet+}$ using eq 7, and these values are also listed in Table 1. For compounds where IE_{gas} data were not available from experiment (2,4,6-trimethylphenol, 2-methylindole, dimethyldisulfide, thioanisole), CBS-QB3 or ROCBS-QB3 IE_{gas} values were used. The resulting $\Delta G^*_{solv,A\bullet+}$ test set differs from previous test sets for solvation models, which do not include open shell species in aqueous solution.

4. RESULTS AND DISCUSSION

According to eq 2 and the thermodynamic cycle shown in Figure 1, the free energy of aqueous oxidation, ΔG^0_{ox}, is given by the sum of the gas-phase ionization energy (IE_{gas}) and the change in free energy of solvation between the neutral (reduced) and the oxidized (radical cation) state ($\Delta\Delta G_{solv}$). In the following sections, we first evaluate CBS-QB3 and selected DFT methods for their prediction of the gas-phase ionization process based on comparisons to experimental IE_{gas} data. We then assess the performance of *a priori* prediction of aqueous oxidation potentials using (RO)CBS-QB3 for ionization energies in combination with all tested implicit solvent models. Finally, we evaluate all tested implicit solvent models for prediction of free energy of solvation of the radical cation species, $\Delta G^*_{solv,A\bullet+}$.

4.1. Performance of DFT Methods and CBS-QB3 for Gas-Phase Adiabatic Ionization Energies. Before considering the condensed phase, we evaluated the applied electronic structure methods for their predictions of gas-phase adiabatic ionization energies of the test set. Existing assessments using high accuracy ionization energy databases such as G2/97[121,122] or its subsets G21IP[123] and IP13[124,125] feature mainly very small molecules. Thus, it is unclear what level of accuracy may be expected for model chemistries that are applied to ionization energy calculations of the larger molecules considered here.

Deviations of computed gas-phase ionization energy with respect to high-accuracy experimental data, at 0 K, are shown in Table 2. CBS-QB3 and M06-2X/aug-cc-pVTZ produced the lowest average errors, exhibiting mean unsigned errors (MUEs) of 0.06 and 0.04 eV respectively. The remaining methods tested (B2PLYP-D/aug-cc-pVTZ, M06-2X/6-31G(d), and B3LYP/aug-cc-PVTZ) all underestimated ionization energies, on average, producing MUEs of 0.18 eV or higher. When applied with a triple-ξ basis set, all three DFT methods (B3LYP, M06-

Table 2. Deviations of Calculated Adiabatic Ionization Energies, IE_{gas} (0 K), from Experimental Values, by Computational Method, in Units of eV[a]

method	MUE	MSE	max dev	
CBS-QB3	0.06	0.03	0.22	DABCO
M06-2X/aug-cc-pVTZ	0.04	0.00	0.16	1,3-dimethoxybenzene
M06-2X/6-31G(d)	0.20	−0.20	0.36	4-phenylenediamine
B2PLYP-D/aug-cc-pVTZ	0.18	−0.11	0.59	4-chlorophenol
B3LYP/aug-cc-pVTZ	0.22	−0.19	0.27	1,4-dimethoxybenzene

[a]MUE refers to the mean unsigned error, MSE refers to the mean signed error. "Maximum deviation" refers to the largest deviation and the compound associated with this deviation. All electronic energies were computed with M06-2X/6-31G(d) geometries except for CBS-QB3 energies, which were determined on geometries optimized using the default B3LYP/6-311G(2d,d,p) method.

dx.doi.org/10.1021/ct4004433 | J. Chem. Theory Comput. 2013, 9, 5046−5058

Table 3. Descriptive Statistics of Solvent Model Performance with Respect to Experimental Values, for Oxidation Potential (E^0_{ox}), Difference in Free Energy of Solvation upon Oxidation ($\Delta\Delta G_{solv}$), Free Energy of Solvation of the Closed-Shell Reduced Species ($\Delta G^*_{solv,A}$), and Free Energy of Solvation of the Oxidized Radical Species ($\Delta G^*_{solv,A\bullet+}$), in Both Aqueous and Acetonitrile Solution, for the Subsets of Compounds Having Available Experimental Values at 298 K (Table 1)[a]

		aqueous				acetonitrile	
solvation model		E^0_{ox}	$\Delta\Delta G_{solv}$	$\Delta G^*_{solv,A}$	$\Delta G^*_{solv,A\bullet+}$	E^0_{ox}	$\Delta\Delta G_{solv}$
SMD	MUE	0.27	0.22	0.03	0.32	0.13	0.13
M06-2X/6-31G(d)	MSE	0.27	0.22	0.00	0.32	−0.04	−0.05
	max dev	0.68	0.62	0.17	0.65	0.29	0.29
SM8	MUE	0.27	0.23	0.04	0.33	0.17	0.18
M06-2X/6-31G(d)	MSE	0.26	0.22	0.02	0.33	−0.13	−0.15
	max dev	0.65	0.59	0.13	0.65	0.35	0.37
COSMO-RS	MUE	0.36	0.32	0.04	0.40	0.17	0.15
BP/cc-pVTZ	MSE	0.35	0.30	0.01	0.39	0.13	0.11
	max dev	0.87	0.81	0.14	0.75	0.39	0.15
IEF-PCM	MUE	0.50	0.45	0.05	0.57	0.24	0.22
M06-2X/6-31G(d)	MSE	0.50	0.45	0.03	0.57	0.24	0.22
	max dev	1.02	0.96	0.15	1.03	0.56	0.55
C-PCM	MUE	0.50	0.46	0.05	0.57	0.24	0.22
M06-2X/6-31G(d)	MSE	0.50	0.46	0.03	0.57	0.24	0.22
	max dev	1.02	0.96	0.15	1.02	0.56	0.55

[a]Values are reported in units of eV for solvation free energy quantities and V (vs SHE) for oxidation potential.

2X, B2PLYP-D) have been previously found to give reasonably accurate geometries and frequencies of small radicals.[126] None of the DFT methods considered here suffered from spin contamination for any of the compounds tested. Adjusted $<S^2>$ values ranged between 0.75 and 0.76 after spin annihilation in all cases.

In previous assessments, these DFT methods exhibited performance roughly similar to that observed here. For a large test set of organic compounds, Fu et al. reported similar average accuracy for ionization energies (0.28 eV) using the B3LYP functional.[127] Other previous assessments have found somewhat smaller average errors for B3LYP; however, those IE_{gas} data sets were composed of atoms and of molecules smaller than those considered here.[91,121,123,128] Applying M06-2X/6-311+G(2df,2p) to the IP13 test set, Zhao and Truhlar[128] reported average errors (2.54 kcal/mol, 0.11 eV) that are larger than average errors we found for M06-2X/aug-cc-pVTZ. This suggests that the very good performance of M06-2X observed here may be fortuitous. As a double hybrid DFT method, B2PLYP-D exhibits slower basis set convergence than single hybrid methods;[87] thus the aug-cc-pVTZ results shown here may underrepresent the accuracy that would be obtained using larger basis sets. Applying B2PLYP-D/(aug-)def2-QZVP to the G21IP test set of atoms and small molecules, Goerigk and Grimme[123] found roughly twice better accuracy (2.3 kcal/mol, 0.10 eV) than we find with B2PLYP-D/aug-cc-pVTZ on the test set reported here.

For the present test set of ionization energies, CBS-QB3 produced errors that are of similar magnitude to those reported in previous studies on atoms and smaller molecules. Of the eighteen compounds for which we found experimental data, CBS-QB3 deviations exceeded 0.1 eV for two compounds (1,3-dimethoxybenzene and DABCO), and the maximum deviation was 0.22 eV (DABCO). When tested against the G2/97 set of ionization energies of atoms and small molecules, CBS-QB3 had an MUE of 4.4 kJ/mol (0.046 eV),[85,91] which is slightly smaller than the average error we found (0.06 eV) for the present data set. CBS-QB3 suffered from spin contamination for several compounds in our set (4-chlorophenol, 4-cyanophenol, anisole, aniline, 4-toluidine, *N*-methylaniline, *N*,*N*′-dimethylaniline, indole, 1-methylindole, 2-methylindole, thioanisole). In cases where $<S^2>$ exceeded 0.80, we performed an additional IE_{gas} calculation using ROCBS-QB3. CBS-QB3 is parametrized to correct for spin contamination with an empirical scaling factor,[85] whereas ROCBS-QB3 does not require this correction. For all cases considered, CBS-QB3 IE_{gas} values agreed with ROCBS-QB3 results to within 0.04 eV or less, indicating that the CBS-QB3 empirical spin contamination correction was adequate for all cases considered here (Table 1). In separate calculations, the T_1 diagnostic[129] (computed using CCSD/6-31+G(d,p)) was found to be >0.02 for several molecules in the test set (4-carboxyphenol, 4-cyanophenol, 4-methoxyphenol, 4-methylphenol, 3,4-dimethoxyphenol, anisole, 1,2-dimethoxybenzene, 1,3-dimethoxybenzene, 1,2,4-trimethoxybenzene, aniline, *N*-methylaniline, *N*,*N*′-dimethylaniline, 2-methylindole). In these cases, problems with the Hartree−Fock reference may account for some of the errors found for CBS-QB3. However, for the compound for which CBS-QB3 gave the least accurate IE_{gas} value, DABCO, the method suffered from neither spin contamination nor apparent difficulty with the reference. Among the methods considered here, CBS-QB3 and ROCBS-QB3 gave results considered sufficiently accurate for gas-phase ionization energies, for the purposes of the present study.

4.2. Performance of Implicit Solvent Models for Single Electron Oxidation Potentials in Water and in Acetonitrile. We computed single-electron oxidation potentials for the entire test set in both aqueous and acetonitrile solvents with the implicit models SM8, SMD, IEF-PCM, C-PCM, and COSMO-RS, via eqs 2−4. CBS-QB3 (or ROCBS-QB3) was used the account for the gas-phase ionization energy, IE_{gas} at 298 K. Predicted oxidation potential values were compared to available experimental data (Table 1), and performance statistics are shown in Tables 3 and 4. SMD performed the best overall, with an MUE of 0.27 V for aqueous oxidation potentials, and an MUE of 0.13 V for oxidation potentials in acetonitrile. IEF-PCM and C-PCM performed the worst, both having MUEs of 0.50 V for $E^0_{ox,aq}$ and 0.24 V for

dx.doi.org/10.1021/ct4004433 | J. Chem. Theory Comput. 2013, 9, 5046−5058

Table 4. Errors in Calculated Oxidation Potentials, by Compound Class, in V, Based on CBS-QB3 (or ROCBS-QB3) Ionization Energies (IE_{gas} (298 K)) and Implicit Model Free Energies of Solvation, Computed Using M06-2X/6-31G(d) To Describe Electronic Structure (or BP/cc-pVTZ, for COSMO-RS), in Aqueous Solution and Acetonitrile

	aqueous					acetonitrile				
	SMD	SM8	COSMO-RS	IEF-PCM	C-PCM	SMD	SM8	COSMO-RS	IEF-PCM	C-PCM
All Compounds	*22 compounds in total*					*19 compounds in total*				
MUE:	0.27	0.27	0.36	0.50	0.50	0.13	0.17	0.17	0.24	0.24
MSE:	0.27	0.26	0.35	0.50	0.50	−0.04	−0.13	0.13	0.24	0.24
max dev:	0.68	0.65	0.87	1.02	1.02	0.29	0.35	0.39	0.56	0.56
Phenols	*7 compounds*					*1 compound*				
MUE:	0.43	0.44	0.51	0.69	0.69	0.22	0.24	0.39	0.46	0.46
MSE:	0.43	0.44	0.51	0.69	0.69	0.22	0.24	0.39	0.46	0.46
max dev:	0.68	0.65	0.87	1.02	1.02	0.22	0.24	0.39	0.46	0.46
Methoxybenzenes	*5 compounds*					*5 compounds*				
MUE:	0.23	0.31	0.41	0.44	0.45	0.12	0.15	0.18	0.19	0.19
MSE:	0.23	0.31	0.41	0.44	0.45	−0.08	−0.12	0.18	0.19	0.19
max dev:	0.32	0.61	0.50	0.56	0.56	0.15	0.20	0.36	0.37	0.37
Anilines	*4 compounds*					*5 compounds*				
MUE:	0.13	0.12	0.14	0.38	0.39	0.10	0.16	0.15	0.26	0.26
MSE:	0.12	0.07	0.06	0.38	0.39	−0.01	−0.16	0.05	0.26	0.26
max dev:	0.24	0.16	0.16	0.52	0.52	0.14	0.35	0.26	0.40	0.40
Indoles	*3 compounds*					*3 compounds*				
MUE:	0.19	0.16	0.26	0.42	0.42	0.04	0.11	0.16	0.23	0.24
MSE:	0.19	0.16	0.26	0.42	0.42	0.00	−0.11	0.16	0.23	0.24
max dev:	0.24	0.19	0.28	0.47	0.47	0.06	0.15	0.18	0.29	0.29
Aliphatic Amines						*4 compounds*				
MUE:						0.25	0.27	0.10	0.20	0.20
MSE:						−0.15	−0.27	0.06	0.20	0.20
max dev:						0.29	0.34	0.26	0.56	0.56
Organosulfurs	*3 compounds*					*1 compound*				
MUE:	0.23	0.14	0.34	0.40	0.40	0.13	0.03	0.31	0.32	0.32
MSE:	0.23	0.14	0.34	0.40	0.40	0.13	0.03	0.31	0.32	0.32
max dev:	0.24	0.19	0.37	0.43	0.43	0.13	0.03	0.31	0.32	0.32

$E^0_{ox,ACN}$. These are noticeably larger errors than that reported by Hodgson et al. for the computed redox potentials of nitroxide structures in water using IEF-PCM (MUE of 0.04 V).[34]

Across the six solute families in the test set (phenols, methoxybenzenes, anilines, indoles, aliphatic amines, organosulfur compounds), the same order of performance of the considered solvent models in either aqueous or acetonitrile solvent was observed, with only a couple of exceptions. For most families, SMD and SM8 performed very similarly, together giving the lowest MUE for prediction of oxidation potentials in solution, followed by COSMO-RS and finally by IEF-PCM and C-PCM, which displayed a near-identical performance throughout (Table 4). However, for aliphatic amines in acetonitrile, the smallest MUE was obtained with COSMO-RS, followed by IEF-PCM and C-PCM, and then SMD and SM8. In the case of anilines in aqueous phase, SM8 had the lowest MUE, followed closely by COSMO-RS and SMD, then IEF-PCM and C-PCM. SM8 delivered slightly smaller MUEs than SMD for the organosulfurs, indoles, and anilines.

Inspection of the errors suggests that prediction skill of all implicit solvent models is worse for oxidation potentials in water compared to those in acetonitrile (Table 4). All five implicit models overpredict nearly all of the aqueous oxidation potential data. In acetonitrile solvent, COSMO-RS, IEF-PCM, and C-PCM overpredict nearly all of the oxidation potentials but to a lesser extent than in aqueous solution. With SMD, nine of the nineteen E^0_{ox} data in acetonitrile solvent were overpredicted, and ten were underpredicted, whereas the other models overpredicted nearly all of the oxidation potentials in acetonitrile. With SM8, nearly all of the E^0_{ox} values in acetonitrile were underpredicted. Within each compound group, the average errors for oxidation potentials calculated in acetonitrile were lower than in aqueous solution for all models (noting that some compounds only had known oxidation potentials within one solvent). Anilines were an exception, for which COSMO-RS errors in acetonitrile solvent were higher than those in aqueous solution.

As a compound class, phenols garnered the worst performance for all methods in either solvent. The best performing method was SMD, with an MUE of 0.43 V for the seven phenol compounds investigated in aqueous phase and a maximum

error of 0.68 V (4-cyanophenol, Table S1). The worst performing methods were C-PCM and IEF-PCM, with MUEs of 0.69 V for phenols. These errors are somewhat higher than those reported by Winget et al., who computed aqueous oxidation potentials for phenols using an older generation solvent model (SM5.42R/BPW91/MIDI!).[4] With the best performing solvent model, SMD, four of the seven phenols considered here had a computed oxidation potential that deviated by more than 0.5 V compared to experiment, indicating that the large MUE for phenols is not attributable to one or two aberrant outliers. These errors cannot be attributed to inaccuracies in the (CBS-QB3) computed or experimental gas-phase ionization energies. Errors in E^0_{ox} values for phenols and most other compounds in the test set must arise largely from the treatment of the solvation energy, and this is discussed further in sections 4.3, 4.4, and 4.5 below. Finally, it is worth noting that the pK_a values for the oxidized phenols are very low (e.g., −2.0 for phenol$^{\bullet+}$)[3] and it is common for phenols to undergo hydrogen atom transfer instead of electron transfer.[130] Thus, formation of the aqueous phenol radical cation is not favored energetically, and this may partly account for the poor performance of implicit solvent models for this species.

Within each compound class, linear regression of computed vs experimental E^0_{ox} values might be used to improve the quality of the prediction for other compounds in the same class. This is apparent by visual inspection of Figure 2. This strategy has been applied in previous studies as a way to correct for systematic biases in implicit solvent models.[4,8,131] However, it is unclear whether such relationships will always give good results, and they are limited to cases where experimental data are available for compounds similar to the compound of interest.

Multiple structural conformers could contribute to the solvated geometry for some solutes, and we did not consider this here. For example, 1,3-dimethoxybenzene, 1,4-dimethoxybenzene, and 4-methoxyphenol have multiple contributing rotamers in the gas phase, and we employed only one conformation. The differences in gas-phase ionization energies among rotamers were not large (1,3-dimethoxybenzene, 0.12 eV;[114] 1,4-dimethoxybenzene, 0.03 eV;[113] 4-methoxyphenol, 0.01 eV[117]). For all solutes, we used the conformation having the lowest experimental adiabatic gas-phase ionization energy, which in these cases were the *trans* conformations, suggesting that intramolecular substituent interactions are not large in the gas phase. Nonetheless, it is imaginable that the lowest energy conformations in solution phase may differ from those in the gas phase for these molecules, and we did not explore this possibility here.

4.3. Performance of Implicit Solvent Models for $\Delta\Delta G_{solv}$ of Oxidation. As shown in Figure 1, $\Delta\Delta G_{solv}$ represents the change in solvation free energy upon oxidation. $\Delta\Delta G_{solv}$ values are extracted directly from reported E^0_{ox} and IE_{gas} values, based on eq 6. Experimental $\Delta\Delta G_{solv}$ values spanned a range of −1.93 eV (1,2,4-trimethoxybenzene) to −3.08 eV (4-cyanophenol) in aqueous solution and −1.69 eV (1,2,4-trimethoxybenzene) to −2.85 eV (*N*-butylamine) in acetonitrile solution (Table 1). Computationally, $\Delta\Delta G_{solv}$ is evaluated as the difference in free energy of solvation between the oxidized and reduced species, as shown in eq 3. Individual computed $\Delta\Delta G_{solv}$ values are listed in Table S2 for each of the methods tested.

Given that CBS-QB3 predicts IE_{gas} values with an average error of 0.06 eV, we can expect that the performances of implicit solvent models for $\Delta\Delta G_{solv}$ are reflected by the performances we found for E^0_{ox}, and indeed this is seen in Table 3. Among the methods we tested here, SMD/M06-2X/aug-cc-pVTZ had the lowest MUE, 0.20 eV, for aqueous $\Delta\Delta G_{solv}$ values (Table 5, Table S2). With MUEs of 0.45 and 0.46 eV in aqueous solution, both IEF-PCM and C-PCM respectively performed more poorly than either the SMx

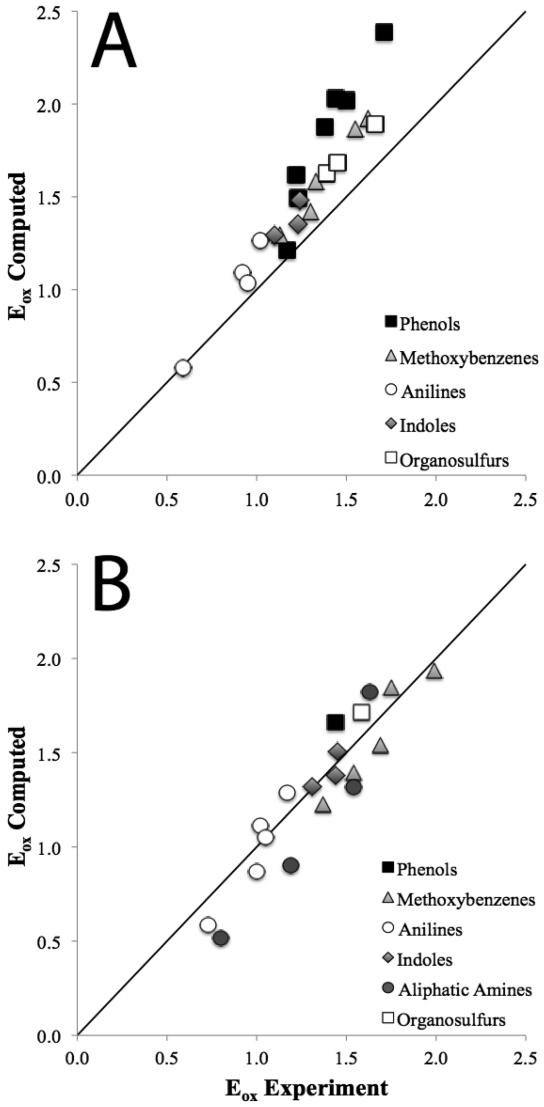

Figure 2. Oxidation potentials computed using CBS-QB3 for IE_{gas} (298 K) and SMD/M06-2X/6-31G(d) for $\Delta\Delta G_{solv}$, compared to experiment, grouped by compound class in V vs SHE. Panel A. Aqueous solution. Panel B. Acetonitrile solvent.

Table 5. Statistics Describing the Deviations of Computation from Experiment for the Change in Free Energy of Solvation upon Oxidation ($\Delta\Delta G_{solv}$) for Different Model Chemistries, in Units of eV, in Aqueous Solution[a]

method	MUE	MSE	max dev	
SMD/M06-2X/6-31G(d)	0.21	0.21	0.61	p-cyanophenol
SMD/M06-2X/aug-cc-pVTZ	0.20	0.18	0.59	p-cyanophenol
SM8/M06-2X/6-31G(d)	0.22	0.20	0.58	p-cyanophenol
SM8/B3LYP/6-31G(d)	0.21	0.19	0.60	p-cyanophenol

[a]All electronic structure calculations were performed with M06-2X/6-31G(d) gas-phase geometries.

dx.doi.org/10.1021/ct4004433 | J. Chem. Theory Comput. 2013, 9, 5046−5058

models or COSMO-RS (Table 3). Consistent with our observations for E^0_{ox}, COSMO-RS performed better than IEF-PCM or C-PCM, but not as well as the SMx models, for aqueous $\Delta\Delta G_{solv}$. These trends are coherent with previous implicit model assessments for solvation free energies of closed shell species. Cramer and Truhlar found that SM8 outperformed IEF-PCM, C-PCM, and COSMO (as implemented in NWChem) when evaluating aqueous solvation free energies of both neutral and ionic closed shell molecules.[61]

All implicit models performed poorly for the $\Delta\Delta G_{solv}$ values of phenol and substituted phenols in water. The worst case for all models is 4-cyanophenol; this compound also exhibits the largest magnitudes in the data set for the three properties, IE_{gas}, $E^0_{ox,aq}$, and $\Delta\Delta G_{solv,aq}$ (Table 1). The largest $\Delta\Delta G_{solv,aq}$ deviation from experiment was 0.96 eV for 4-cyanophenol, with the IEF-PCM and C-PCM models (Table S2).

All implicit models exhibited similar performance, on average, for $\Delta\Delta G_{solv}$ in acetonitrile solvent, with MUEs ranging from 0.13 to 0.22 eV (Table 3). The best performing method was SMD, with an MUE of 0.13 eV and a maximum deviation of 0.29 eV (triethylamine) (Table S2). Applying the SMD solvation model to reduction potentials or organic molecules, Sviatenko et al. reported errors in $\Delta\Delta G_{solv}$ values similar to those found here; they observed MUEs between 0.17 and 0.31 eV across reductions of three classes of compounds (nitroaromatics, quinones, azocyclics) in three different solvents (water, acetonitrile, DMF).[42]

Implicit solvent model results did not exhibit a strong dependence on electronic structure method or basis set. $\Delta\Delta G_{solv,aq}$ computations with SMD using different DFT methods (M06-2X, B3LYP) and basis sets (6-31G(d), aug-cc-PVTZ) suggest that computed $\Delta\Delta G_{solv,aq}$ values are not highly sensitive to the model chemistry or basis set used (Table 5, Table S2), as long as the distribution of molecular charge separation is correct. This is consistent with findings of Marenich et al., who observed only weak dependence of solvation free energy on model chemistry and basis set for neutral and cationic species using SMD.[31]

The underlying origins of successes or failures of implicit solvent models are not easily explained. Additionally, it is unclear whether implicit models, which are empirically parametrized, may properly account for specific radical-solvent interactions[132] or associated solvent structuring in either acetonitrile or water.

To gain further insight into the performance of implicit solvent models for the oxidized open-shell species, we apportioned aqueous $\Delta\Delta G_{solv}$ values into the contributions from the neutral ($\Delta G^*_{solv,A}$) and radical cation species ($\Delta G^*_{solv,A\bullet+}$), discussed below.

4.4. Performance of Implicit Solvent Models for $\Delta G^*_{solv,A}$. Experimental values of aqueous $\Delta G^*_{solv,A}$ data are shown in Table 1. All implicit solvent models predicted $\Delta G^*_{solv,A}$ with an average error of 0.05 eV or less (Table 3). Overall, the solvation free energy errors for the neutral compounds were relatively small except for the case of DABCO, for which all but one solvation method (COSMO-RS) showed deviations from experiment greater than 0.1 eV. SMD had the lowest error for $\Delta G^*_{solv,A}$, on average, with an MUE of 0.03 eV (Table 3, Table S3). These results are comparable to those of previous studies. Using SMD/M05-2X/6-31G(d), Marenich et al. reported an accuracy similar to that found here for SMD, reporting an MUE of 0.59 kcal/mol (0.026 eV) for aqueous solubilities of a test set of neutral compounds.[31] The average error of SM8 for the present aqueous $\Delta G^*_{solv,A}$ data set was slightly higher than that reported by Cramer and Truhlar, who observed an MUE of 0.55 kcal/mol (0.023 eV) using SM8/mPW1PW/6-31G(d) for a large test set of neutral molecules.[61] For the SAMPL2 data set of organic compounds having size comparable to those considered here, errors in solvation free energy were found to be slightly larger, 1.33 kcal/mol (0.06 eV) and 2.61 kcal/mol (0.11 eV), respectively, for SM8 and SMD using M06-2X/6-31G(d). IEF-PCM performance for aqueous $\Delta G^*_{solv,A}$ values of our data set was slightly worse than that reported by Cramer and Truhlar, who found an MUE of 4.87 kcal/mol (0.021 eV) using mPW1PW/6-31G(d). Using HF/6-31G(d) with C-PCM and IEF-PCM, Kelly et al. reported MUEs of 1.11 kcal/mol (0.048 eV) and 1.10 kcal/mol (0.048 eV), respectively, for a test set of aqueous $\Delta G^*_{solv,A}$ data.[29]

4.5. Performance of Implicit Solvent Models for $\Delta G^*_{solv,A\bullet+}$. Experimental values of the aqueous solvation free energy of the open shell oxidized species, $\Delta G^*_{solv,A\bullet+}$, were determined using eq 7; these data are shown in Table 1. SMD and SM8 produced the lowest average error for $\Delta G^*_{solv,A\bullet+}$, with MUEs of 0.32 and 0.33 eV, respectively (Table 3, S4). IEF-PCM and C-PCM gave average errors roughly twice as large, with MUEs of 0.57 eV for $\Delta G^*_{solv,A\bullet+}$ for both models. COSMO-RS fell in between these models, with an MUE of 0.40 eV. For the aqueous solvation free energies of a set of closed-shell organic anions and cations, as well as water clusters containing ions, Cramer and Truhlar reported MUEs of 3.2 kcal/mol (0.14 eV) for SM8 and 12.4 kcal/mol (0.54 eV) for IEF-PCM.[61] Takano and Houk found MUEs in solvation free energy of 3.0 kcal/mol (0.13 eV) for a set of thirteen charged (anionic/cationic) species using C-PCM and compared that with reported larger errors (7.5 kcal/mol, 0.33 eV) for an SMx model (SM5.42R) and 9.15 kcal/mol (0.40 eV) for COSMO.[62] The newer generations of the SMx models have been parametrized to produce improved values of solvation free energies for charged species, having reported average errors of 3.7 kcal/mol (0.16 eV) for SMD/M05-2X/6-31G(d) and 4.31 kcal/mol (0.19 eV) for SM8/mPW1PW/6-31G(d)) for ΔG^*_{solv} of closed shell charged (anionic/cationic) species.[30,31] The results in this study for $\Delta G^*_{solv,A\bullet+}$ are thus similar to errors found for the same models when applied to closed shell cations in water.

It is unclear how to interpret the apparent prediction skill of implicit solvent models for $\Delta G^*_{solv,A\bullet+}$ values of the compound set considered here. While observed errors are consistent with average errors previously reported for these models for the solvation free energy values of monovalent cations, additional uncertainties may arise from the specific radical-solvent interactions contributing to $\Delta G^*_{solv,A\bullet+}$. Preliminary evidence indicates that these interactions may differ in strength compared to analogous closed-shell-cation-solvent interactions.[132,133] This may contribute additional uncertainty to the solvent models, which were not parametrized with data involving radicals.

Taking into consideration the relatively small uncertainties for prediction of IE_{gas} (0.06 eV) and $\Delta G^*_{solv,A}$ (0.03 to 0.05 eV), we attributed the dominant source of error in single-electron aqueous oxidation potential computations to the computation of $\Delta G^*_{solv,A\bullet+}$, which is consistent with previous interpretations.[4,8] This is corroborated by the observation that errors in computed $\Delta G^*_{solv,A\bullet+}$ values are similar in magnitude (once

converted from eV to V by the Nernst equation) to errors for computed E^0_{ox} values (Table 3).

5. IMPLICATIONS AND RECOMMENDATIONS

In this study, we assess five implicit solvent models for their ability to predict oxidation potentials of a set of neutral organic compounds in aqueous and acetonitrile solvents. We additionally apportion these results into contributions arising from the gas-phase ionization energy, IE_{gas}, and the change in solvation energy upon oxidation, $\Delta\Delta G_{solv}$. We find that contemporary implicit solvent models produce average errors in $\Delta\Delta G_{solv}$ ranging from 0.22 to 0.46 eV in aqueous solvent. To our knowledge, this is the first study to compile a test set of experimental values for the free energy of solvation of the radical cation species, $\Delta G^*_{solv,A\bullet+}$, for several organic compounds in aqueous solution.

For aqueous E^0_{ox} calculations, the predominant source of error is the treatment of the solvation free energy of the radical open-shell species, $\Delta G^*_{solv,A\bullet+}$, which erred by 0.32 eV, on average, with the SMD solvent model, and by 0.33 eV with SM8, by 0.49 eV with COSMO-RS, and by 0.57 eV, on average, for both the IEF-PCM and C-PCM solvent models.

Based on results obtained for IE_{gas} and $\Delta\Delta G_{solv}$, we formulated a "best method" for the computation of oxidation potentials with implicit models. We chose an electronic structure method considered reliable for IE_{gas}, (RO)CBS-QB3, and we combined this together with the solvent model having the lowest average error for $\Delta\Delta G_{solv}$ (SMD). Thus, the recommended method to compute the oxidation potential relative to SHE is

$$E^0_{ox} = -\left[\frac{-(IE_{gas^{298\,K}_{CBS\text{-}QB3}} + \Delta\Delta G_{solv,SMD})}{nF} + \mathrm{SHE}\right] \quad (8)$$

Oxidation potentials calculated by eq 8 had an MUE of 0.27 V for aqueous solvent, with a maximum deviation of 0.68 V (4-cyanophenol), and an MUE of 0.13 V for acetonitrile solvent with a maximum deviation of 0.29 V (DABCO) for the test set considered here (Table 3, 4). In cases where CBS-QB3 exhibits significant spin contamination, ROCBS-QB3 is recommended as an alternative for computing IE_{gas}.[91] Eq 8 turns out to be the same formulation recently applied by Psciuk et al. in their theoretical study of redox potentials of nucleic acid bases.[11]

Further improvements in models describing solvation energies of charged open shell species would aid in predictions of oxidation potentials and related thermodynamic properties. In "cluster-continuum" approaches, one or more explicit solvent molecules are placed around the solute, and the resulting cluster is embedded in an implicit solvent model.[76] This strategy has been suggested to improve computed solvation free energies, redox potentials, and pK_a values.[29,70,76,77,134] By including one explicit water molecule, Winget et al. reported improvements in oxidation potential computations by 30% for phenols using SM5.42R.[4] However, our preliminary calculations (not shown) suggest that it is not trivial to determine the appropriate geometric configurations of explicit molecules around highly delocalized organic open-shell species such as those considered in this study. Even when only a single explicit water molecule is employed, resulting clusters frequently exhibit low potential energy gradients and several relevant potential energy minima. This contrasts with previously published applications of the cluster-continuum approach for the determination of solvation free energies of monatomic ions or for the determination of pK_a values; in these cases, the full ionic charge is highly localized, producing only a limited number of relevant conformations for immediately adjacent explicit water molecules. Additionally, when handling solvated clusters involving open-shell species, careful attention should be paid to choosing an appropriate electronic structure method.[132] Future investigations into methods for determining the appropriate configurations and number of explicit molecules may prove useful in obtaining improved results for redox potentials. The present work provides a baseline assessment of implicit solvent models for the prediction of aqueous oxidation potential for neutral compounds, as well as a benchmark test set of vetted experimental data that may be used in future efforts to design improved modeling approaches.

■ ASSOCIATED CONTENT

Supporting Information

Computed oxidation potentials in aqueous or acetonitrile solvents computed from (RO)CBS-QB3 gas-phase ionization energies and SMD/M06-2X/6-31G(d) free energies of solvation, $\Delta\Delta G_{solv}$ and $\Delta G^*_{solv,A\bullet+,aq}$ errors for each solvation model used and comparison of $\Delta G^*_{solv,A,aq}$ to experiment for each compound within the test set are listed. This material is available free of charge via the Internet at http://pubs.acs.org.

■ AUTHOR INFORMATION

Corresponding Author

*E-mail: samuel.arey@epfl.ch.

Author Contributions

The manuscript was written through contributions of all authors. All authors have given approval to the final version of the manuscript.

Notes

The authors declare no competing financial interest.

■ ACKNOWLEDGMENTS

The authors thank Silvio Canonica and Peter R. Tentscher for helpful discussions. We also gratefully acknowledge three anonymous reviewers for their valuable comments. This study was supported by U.S. NSF IRFP award # 0852999, Swiss National Fund Project Grant 200021-126893, and the Swiss National Super Computing Center (CSCS).

■ REFERENCES

(1) Canonica, S.; Hellrung, B.; Müller, P.; Wirz, J. *Environ. Sci. Technol.* **2006**, *40*, 6636−6641.
(2) Wenk, J.; von Gunten, U.; Canonica, S. *Environ. Sci. Technol.* **2011**, *45*, 1334−1340.
(3) Canonica, S.; Hellrung, B.; Wirz, J. *J. Phys. Chem. A* **2000**, *104*, 1226−1232.
(4) Winget, P.; Cramer, C. J.; Truhlar, D. G. *Theor. Chem. Acc.* **2004**, *112*, 217−227.
(5) Paukku, Y.; Hill, G. *J. Phys. Chem. A* **2011**, *115*, 4804−4810.
(6) Riahi, S.; Norouzi, P.; Bayandori Moghaddam, A.; Ganjali, M. R.; Karimipour, G. R.; Sharghi, H. *Chem. Phys.* **2007**, *337*, 33−38.
(7) Reynolds, C. A. *J. Am. Chem. Soc.* **1990**, *112*, 7545−7551.
(8) Winget, P.; Weber, E. J.; Cramer, C. J.; Truhlar, D. G. *Phys. Chem. Chem. Phys.* **2000**, *2*, 1231−1239.
(9) Shi, J.; Zhao, Y.-L.; Wang, H.-J.; Rui, L.; Guo, Q.-X. *J. Mol. Struct.: THEOCHEM* **2009**, *902*, 66−71.
(10) Fiser, B.; Szori, M.; Jójárt, B.; Izsák, R.; Csizmadia, I. G.; Viskolcz, B. *J. Phys. Chem. B* **2011**, *115*, 11269−11277.
(11) Psciuk, B. T.; Lord, R. L.; Munk, B. H.; Schlegel, H. B. *J. Chem. Theory Comput.* **2012**, *8*, 5107−5123.

(12) Wardman, P. *J. Phys. Chem. Ref. Data* **1989**, *18*, 1637−1755.
(13) Jonsson, M.; Lind, J.; Eriksen, T. E.; Merényi, G. *J. Am. Chem. Soc.* **1994**, *116*, 1423−1427.
(14) Jonsson, M.; Lind, J.; Reitberger, T.; Eriksen, T. E.; Merényi, G. *J. Phys. Chem.* **1993**, *97*, 11278−11282.
(15) Merényi, G.; Lind, J.; Shen, X. *J. Phys. Chem.* **1988**, *92*, 134−137.
(16) Neta, P. *J. Chem. Educ.* **1981**, *58*, 110−113.
(17) Meisel, D.; Neta, P. *J. Am. Chem. Soc.* **1975**, *97*, 5198−5203.
(18) Meisel, D.; Neta, P. *J. Phys. Chem.* **1975**, *79*, 2459−2461.
(19) Jonsson, M.; Wayner, D. D. M.; Lusztyk, J. *J. Phys. Chem.* **1996**, *100*, 17539−17543.
(20) Lind, J.; Shen, X.; Eriksen, T. E.; Merényi, G. *J. Am. Chem. Soc.* **1990**, *112*, 479−482.
(21) Cramer, C. J.; Truhlar, D. G. *Chem. Rev.* **1999**, *99*, 2161−2200.
(22) Cramer, C. J. *Essentials of Computational Chemistry: Theories and Models*, 2nd ed.; John Wiley & Sons Ltd.: West Sussex, 2004; 596 pp.
(23) Mennucci, B.; Cancès, E.; Tomasi, J. *J. Phys. Chem. B* **1997**, *101*, 10506−10517.
(24) Cancès, E.; Mennucci, B.; Tomasi, J. *J. Chem. Phys.* **1997**, *107*, 3032.
(25) Cancès, E.; Mennucci, B. *J. Math. Chem.* **1998**, *23*, 309−326.
(26) Klamt, A.; Schüürmann, G. *J. Chem. Soc., Perkin Trans. 2* **1993**, 799−805.
(27) Cossi, M.; Rega, N.; Scalmani, G.; Barone, V. *J. Comput. Chem.* **2003**, *24*, 669−681.
(28) Barone, V.; Cossi, M. *J. Phys. Chem. A* **1998**, *102*, 1995−2001.
(29) Kelly, C. P.; Cramer, C. J.; Truhlar, D. G. *J. Chem. Theory Comput.* **2005**, *1*, 1133−1152.
(30) Marenich, A. V.; Olson, R. M.; Kelly, C. P.; Cramer, C. J.; Truhlar, D. G. *J. Chem. Theory Comput.* **2007**, *3*, 2011−2033.
(31) Marenich, A. V.; Cramer, C. J.; Truhlar, D. G. *J. Phys. Chem. B* **2009**, *113*, 6378−6396.
(32) Klamt, A. *J. Phys. Chem.* **1995**, *99*, 2224−2235.
(33) Klamt, A.; Jonas, V.; Bürger, T.; Lohrenz, J. C. W. *J. Phys. Chem. A* **1998**, *102*, 5074−5085.
(34) Hodgson, J. L.; Namazian, M.; Bottle, S. E.; Coote, M. L. *J. Phys. Chem. A* **2007**, *111*, 13595−13605.
(35) Namazian, M.; Zare, H. R.; Coote, M. L. *Biophys. Chem.* **2008**, *132*, 64−68.
(36) Zubatyuk, R. I.; Gorb, L.; Shishkin, O. V.; Qasim, M.; Leszczynski, J. *J. Comput. Chem.* **2010**, *31*, 144−150.
(37) Lewis, A.; Bumpus, J. A.; Truhlar, D. G.; Cramer, C. J. *J. Chem. Educ.* **2004**, *81*, 596−604.
(38) Namazian, M.; Almodarresieh, H. A. *J. Mol. Struct.: THEOCHEM* **2004**, *686*, 97−102.
(39) Namazian, M.; Almodarresieh, H. A.; Noorbala, M. R.; Zare, H. R. *Chem. Phys. Lett.* **2004**, *396*, 424−428.
(40) Shamsipur, M.; Alizadeh, K.; Arshadi, S. *J. Mol. Struct.: THEOCHEM* **2006**, *758*, 71−74.
(41) Bylaska, E. J.; Salter-Blanc, A. J.; Tratnyek, P. G. Aquatic Redox Chemistry. *ACS Symposium Series*: American Chemical Society: Washington, DC, 2011; Vol. *1071*, pp 37−64.
(42) Sviatenko, L.; Isayev, O.; Gorb, L.; Hill, F.; Leszczynski, J. *J. Comput. Chem.* **2011**, *32*, 2195−2203.
(43) Cwiertny, D. M.; Arnold, W. A.; Kohn, T.; Rodenburg, L. A.; Roberts, A. L. *Environ. Sci. Technol.* **2010**, *44*, 7928−7936.
(44) Solntsev, K. M.; Ghosh, D.; Amador, A.; Josowicz, M.; Krylov, A. I. *J. Phys. Chem. Lett.* **2011**, *2*, 2593−2597.
(45) Tugsuz, T. *J. Phys. Chem. B* **2010**, *114*, 17092−17101.
(46) Assary, R. S.; Curtiss, L. A.; Redfern, P. C.; Zhang, Z.; Amine, K. *J. Phys. Chem. C* **2011**, *115*, 12216−12223.
(47) Camarada, M. B.; Jaque, P.; Díaz, F. R.; del Valle, M. A. *J. Polym. Sci., Part B: Polym. Phys.* **2011**, *49*, 1723−1733.
(48) Namazian, M.; Coote, M. L. *J. Phys. Chem. A* **2007**, *111*, 7227−7232.
(49) Blinco, J. P.; Hodgson, J. L.; Morrow, B. J.; Walker, J. R.; Will, G. D.; Coote, M. L.; Bottle, S. E. *J. Org. Chem.* **2008**, *73*, 6763−6771.
(50) Lin, C. Y.; Coote, M. L.; Gennaro, A.; Matyjaszewski, K. *J. Am. Chem. Soc.* **2008**, *130*, 12762−12774.
(51) Namazian, M.; Lin, C. Y.; Coote, M. L. *J. Chem. Theory Comput.* **2010**, *6*, 2721−2725.
(52) Liptak, M. D.; Gross, K. C.; Seybold, P. G.; Feldgus, S.; Shields, G. C. *J. Am. Chem. Soc.* **2002**, *124*, 6421−6427.
(53) Liptak, M. D.; Shields, G. C. *Int. J. Quantum Chem.* **2001**, *85*, 727−741.
(54) Magill, A. M.; Cavell, K. J.; Yates, B. F. *J. Am. Chem. Soc.* **2004**, *126*, 8717−8724.
(55) Sadlej-Sosnowska, N. *Theor. Chem. Acc.* **2007**, *118*, 281−293.
(56) Verdolino, V.; Cammi, R.; Munk, B. H.; Schlegel, H. B. *J. Phys. Chem. B* **2008**, *112*, 16860−16873.
(57) Casasnovas, R.; Frau, J.; Ortega-Castro, J.; Salvà, A.; Donoso, J.; Muñoz, F. *J. Mol. Struct.: THEOCHEM* **2009**, *912*, 5−12.
(58) Fu, Y.; Liu, L.; Li, R.-Q.; Liu, R.; Guo, Q.-X. *J. Am. Chem. Soc.* **2004**, *126*, 814−822.
(59) Li, J.-N.; Fu, Y.; Liu, L.; Guo, Q.-X. *Tetrahedron* **2006**, *62*, 11801−11813.
(60) Yu, A.; Liu, Y.; Li, Z.; Cheng, J.-P. *J. Phys. Chem. A* **2007**, *111*, 9978−9987.
(61) Cramer, C. J.; Truhlar, D. G. *Acc. Chem. Res.* **2008**, *41*, 760−768.
(62) Takano, Y.; Houk, K. N. *J. Chem. Theory Comput.* **2005**, *1*, 70−77.
(63) Klamt, A.; Eckert, F.; Diedenhofen, M. *J. Phys. Chem. B* **2009**, *113*, 4508−4510.
(64) Klamt, A.; Diedenhofen, M. *J. Comput.-Aided Mol. Des.* **2010**, *24*, 357−360.
(65) Reinisch, J.; Klamt, A.; Diedenhofen, M. *J. Comput.-Aided Mol. Des.* **2012**, *26*, 669−673.
(66) Marenich, A. V.; Cramer, C. J.; Truhlar, D. G. *J. Phys. Chem. B* **2009**, *113*, 4538−4543.
(67) Ribeiro, R. F.; Marenich, A. V.; Cramer, C. J.; Truhlar, D. G. *J. Comput.-Aided Mol. Des.* **2010**, *24*, 317−333.
(68) Soteras, I.; Orozco, M.; Luque, F. J. *J. Comput.-Aided Mol. Des.* **2010**, *24*, 281−291.
(69) Sulea, T.; Wanapun, D.; Dennis, S.; Purisima, E. O. *J. Phys. Chem. B* **2009**, *113*, 4511−4520.
(70) Ho, J.; Coote, M. L. *Theor. Chem. Acc.* **2010**, *125*, 3−21.
(71) Tannor, D. J.; Marten, B.; Murphy, R.; Friesner, R. A.; Sitkoff, D.; Nicholls, A.; Honig, B.; Ringnalda, M.; Goddard, W. A. *J. Am. Chem. Soc.* **1994**, *116*, 11875−11882.
(72) Marten, B.; Kim, K.; Cortis, C.; Friesner, R. A.; Murphy, R. B.; Ringnalda, M. N.; Sitkoff, D.; Honig, B. *J. Phys. Chem.* **1996**, *100*, 11775−11788.
(73) Truong, T. N.; Stefanovich, E. V. *Chem. Phys. Lett.* **1995**, *240*, 253−260.
(74) Truong, T. N.; Stefanovich, E. V. *J. Chem. Phys.* **1995**, *103*, 3709−3717.
(75) Foresman, J. B.; Keith, T. A.; Wiberg, K. B.; Snoonian, J.; Frisch, M. J. *J. Phys. Chem.* **1996**, *100*, 16098−16104.
(76) Bryantsev, V. S.; Diallo, M. S.; Goddard, W. A., III *J. Phys. Chem. B* **2008**, *112*, 9709−9719.
(77) Jagoda-Cwiklik, B.; Slavíček, P.; Cwiklik, L.; Nolting, D.; Winter, B.; Jungwirth, P. *J. Phys. Chem. A* **2008**, *112*, 3499−3505.
(78) Mohr, P. J.; Taylor, B. N.; Newell, D. B. "The 2010 CODATA recommended values of physical constants" Web version 6.0, 2011. http://physics.nist.gov/constants (accessed March 19, 2013).
(79) Truhlar, D. G.; Cramer, C. J.; Lewis, A.; Bumpus, J. A. *J. Chem. Educ.* **2007**, *84*, 934.
(80) Bartmess, J. E. *J. Phys. Chem.* **1994**, *98*, 6420−6424.
(81) Zhao, Y.; Truhlar, D. G. *Theor. Chem. Acc.* **2008**, *120*, 215−241.
(82) Hehre, W. J. *J. Chem. Phys.* **1972**, *56*, 2257−2261.
(83) Hariharan, P. C.; Pople, J. A. *Theor. Chem. Acc.* **1973**, *28*, 213−222.
(84) Frisch, M. J.; Trucks, G. W.; Schlegel, H. B.; Scuseria, G. E.; Robb, M. A.; Cheeseman, J. R.; Scalmani, G.; Barone, V.; Mennucci, B.; Petersson, G. A.; Nakatsuji, H.; Caricato, M.; Li, X.; Hratchian, H. P.; Izmaylov, A. F.; Bloino, J.; Zheng, G.; Sonnenberg, J. L.; Hada, M.;

Ehara, M.; Toyota, K.; Fukuda, R.; Hasegawa, J.; Ishida, M.; Nakajima, T.; Honda, Y.; Kitao, O.; Nakai, H.; Vreven, T.; Montgomery, J. A., Jr.; Peralta, J. E.; Ogliaro, F.; Bearpark, M.; Heyd, J. J.; Brothers, E.; Kudin, K. N.; Staroverov, V. N.; Kobayashi, R.; Normand, J.; Raghavachari, K.; Rendell, A.; Burant, J. C.; Iyengar, S. S.; Tomasi, J.; Cossi, M.; Rega, N.; Millam, J. M.; Klene, M.; Knox, J. E.; Cross, J. B.; Bakken, V.; Adamo, C.; Jaramillo, J.; Gomperts, R.; Stratmann, R. E.; Yazyev, O.; Austin, A. J.; Cammi, R.; Pomelli, C.; Ochterski, J. W.; Martin, R. L.; Morokuma, K.; Zakrzewski, V. G.; Voth, G. A.; Salvador, P.; Dannenberg, J. J.; Dapprich, S.; Daniels, A. D.; Farkas, Ö.; Foresman, J. B.; Ortiz, J. V.; Cioslowski, J.; Fox, D. J. *Gaussian 09, Revision B.01*; Gaussian, Inc.: Wallingford, CT, 2009.

(85) Montgomery, J. A.; Frisch, M. J.; Ochterski, J. W.; Petersson, G. A. *J. Chem. Phys.* **1999**, *110*, 2822−2827.

(86) Montgomery, J. A.; Frisch, M. J.; Ochterski, J. W.; Petersson, G. A. *J. Chem. Phys.* **2000**, *112*, 6532−6542.

(87) Grimme, S. *J. Chem. Phys.* **2006**, *124*, article no. 034108, 16 p.

(88) Schwabe, T.; Grimme, S. *Phys. Chem. Chem. Phys.* **2007**, *9*, 3397−3406.

(89) Kendall, R. A.; Dunning, T. H.; Harrison, R. J. *J. Chem. Phys.* **1992**, *96*, 6796−5652.

(90) Becke, A. D. *J. Chem. Phys.* **1993**, *98*, 5648.

(91) Wood, G. P. F.; Radom, L.; Petersson, G. A.; Barnes, E. C.; Frisch, M. J.; Montgomery, J. A. *J. Chem. Phys.* **2006**, *125*, article no. 094106, 16 p.

(92) Hill, T. L. *An Introduction to Statistical Thermodynamics*; Dover Publications: Reading, MA, 1986; 508 pp.

(93) Merrick, J. P.; Moran, D.; Radom, L. *J. Phys. Chem. A* **2007**, *111*, 11683−11700.

(94) Shao, Y.; Molnar, L. F.; Jung, Y.; Kussmann, J. R.; Ochsenfeld, C.; Brown, S. T.; Gilbert, A. T. B.; Slipchenko, L. V.; Levchenko, S. V.; O Neill, D. P.; DiStasio, R. A., Jr.; Lochan, R. C.; Wang, T.; Beran, G. J. O.; Besley, N. A.; Herbert, J. M.; Lin, C. Y.; Van Voorhis, T.; Chien, S. H.; Sodt, A.; Steele, R. P.; Rassolov, V. A.; Maslen, P. E.; Korambath, P. P.; Adamson, R. D.; Austin, B.; Baker, J.; Byrd, E. F. C.; Dachsel, H.; Doerksen, R. J.; Dreuw, A.; Dunietz, B. D.; Dutoi, A. D.; Furlani, T. R.; Gwaltney, S. R.; Heyden, A.; Hirata, S.; Hsu, C.-P.; Kedziora, G.; Khalliulin, R. Z.; Klunzinger, P.; Lee, A. M.; Lee, M. S.; Liang, W.; Lotan, I.; Nair, N.; Peters, B.; Proynov, E. I.; Pieniazek, P. A.; Rhee, Y. M.; Ritchie, J.; Rosta, E.; Sherrill, C. D.; Simmonett, A. C.; Subotnik, J. E.; Woodcock, H. L., III; Zhang, W.; Bell, A. T.; Chakraborty, A. K.; Chipman, D. M.; Keil, F. J.; Warshel, A.; Hehre, W. J.; Schaefer, H. F., III; Kong, J.; Krylov, A. I.; Gill, P. M. W.; Head-Gordon, M. *Phys. Chem. Chem. Phys.* **2006**, *8*, 3172−3191.

(95) Pye, C. C.; Ziegler, T.; van Lenthe, E.; Louwen, J. N. *Can. J. Chem.* **2009**, *87*, 790−797.

(96) te Velde, G.; Bickelhaupt, F. M.; Baerends, E. J.; Fonseca Guerra, C.; van Gisbergen, S. J. A.; Snijders, J. G.; Ziegler, T. *J. Comput. Chem.* **2001**, *22*, 931−967.

(97) Fonseca Guerra, C.; Snijders, J. G.; te Velde, G.; Baerends, E. J. *Theor. Chem. Acc.* **1998**, *99*, 391−403.

(98) Becke, A. D. *Phys. Rev. A* **1988**, *38*, 3098−3100.

(99) Perdew, J. *Phys. Rev. B* **1986**, *33*, 8822−8824.

(100) Suatoni, J. C.; Snyder, R. E.; Clark, R. O. *Anal. Chem.* **1961**, *33*, 1894−1897.

(101) *Physical/Chemical Property Database (PHYSPROP)*; SRC Environmental Science Center: Syracuse, NY, 2013. http://www.syrres.com (accessed March 20, 2013).

(102) Holton, D. M.; Murphy, D. *J. Chem. Soc., Faraday Trans. 2* **1979**, *75*, 1637−1642.

(103) Huang, L. C. L.; Lin, J. L.; Tzeng, W. B. *Chem. Phys.* **2000**, *261*, 449−455.

(104) Shivatare, V.; Wu, C. H.; Tzeng, W. B. *J. Photochem. Photobiol. A: Chem.* **2013**, *251*, 94−99.

(105) Huang, J.; Huang, K.; Liu, S.; Luo, Q.; Tzeng, W. *J. Photochem. Photobiol., A* **2008**, *193*, 245−253.

(106) Li, C.; Pradhan, M.; Tzeng, W. B. *Chem. Phys. Lett.* **2005**, *411*, 506−510.

(107) Lin, J. L.; Tzeng, W. B. *Chem. Phys. Lett.* **2003**, *377*, 620−626.

(108) Vondrák, T.; Sato, S.-I.; Kimura, K. *J. Phys. Chem. A* **1997**, *101*, 2384−2389.

(109) Lin, J. L.; Tzeng, W. B. *J. Chem. Phys.* **2001**, *115*, 743−751.

(110) Pradhan, M.; Li, C.; Lin, J. L.; Tzeng, W. B. *Chem. Phys. Lett.* **2005**, *407*, 100−104.

(111) Lin, J. L.; Lin, K. C.; Tzeng, W. B. *J. Phys. Chem. A* **2002**, *106*, 6462−6468.

(112) Lin, J. L.; Li, C.; Tzeng, W. B. *J. Chem. Phys.* **2004**, *120*, 10513−10519.

(113) Lin, J. L.; Huang, L. C. L.; Tzeng, W. B. *J. Phys. Chem. A* **2001**, *105*, 11455−11461.

(114) Yang, S. C.; Huang, S. W.; Tzeng, W. B. *J. Phys. Chem. A* **2010**, *114*, 11144−11152.

(115) Watkins, M. J.; Cockett, M. C. R. *J. Chem. Phys.* **2000**, *113*, 10560−10571.

(116) Wu, R. H.; Lin, J. L.; Lin, J.; Yang, S. C.; Tzeng, W. B. *J. Chem. Phys.* **2003**, *118*, 4929.

(117) Li, C.; Su, H.; Tzeng, W. B. *Chem. Phys. Lett.* **2005**, *410*, 99−103.

(118) *NIST Standard Reference Database Number 69*; Linstrom, P. J., Mallard, W. G., Eds.; National Institute of Standards and Technology: Gaithersburg, MD. http://webbook.nist.gov (accessed January 18, 2013).

(119) *CRC Handbook of Chemistry and Physics*; Haynes, W. M., Ed.; CRC Press: Boca Raton, FL; pp 10−200−10−217.

(120) Marenich, A. V.; Kelly, C. P.; Thompson, J. D.; Hawkins, G. D.; Chambers, C. C.; Giesen, D. J.; Winget, P.; Cramer, C. J.; Truhlar, D. G. *Minnesota Solvation Database - version 2012*; University of Minnesota: Minneapolis, 2012. http://comp.chem.umn.edu/mnsol (accessed April 2, 2012).

(121) Curtiss, L. A.; Redfern, P. C.; Raghavachari, K.; Pople, J. A. *J. Chem. Phys.* **1998**, *109*, 42−55.

(122) Curtiss, L. A.; Raghavachari, K.; Redfern, P. C.; Rassolov, V.; Pople, J. A. *J. Chem. Phys.* **1998**, *109*, 7764−7776.

(123) Goerigk, L.; Grimme, S. *J. Chem. Theory Comput.* **2010**, *6*, 107−126.

(124) Lynch, B. J.; Truhlar, D. G. *J. Phys. Chem. A* **2003**, *107*, 3898−3906.

(125) Zhao, Y.; Truhlar, D. G. *J. Phys. Chem. A* **2005**, *109*, 5656−5667.

(126) Tentscher, P. R.; Arey, J. S. *J. Chem. Theory Comput.* **2012**, *8*, 2165−2179.

(127) Fu, Y.; Liu, L.; Yu, H.-Z.; Wang, Y.-M.; Guo, Q.-X. *J. Am. Chem. Soc.* **2005**, *127*, 7227−7234.

(128) Zhao, Y.; Truhlar, D. G. *J. Chem. Theory Comput.* **2008**, *4*, 1849−1868.

(129) Lee, T. J.; Taylor, P. R. *Int. J. Quantum Chem.* **2009**, *36*, 199−207.

(130) Warren, J. J.; Tronic, T. A.; Mayer, J. M. *Chem. Rev.* **2010**, *110*, 6961−7001.

(131) Tentscher, P. R.; Eustis, S. N.; McNeill, K.; Arey, J. S. *Chem.—Eur. J.* **2013**, *19*, 11216−11223.

(132) Tentscher, P. R.; Arey, J. S. *J. Chem. Theory Comput.* **2013**, *9*, 1568−1579.

(133) Tentscher, P. R.; Arey, J. S. *J. Phys. Chem. A.*, submitted for publication.

(134) Marenich, A. V.; Majumdar, A.; Lenz, M.; Cramer, C. J.; Truhlar, D. G. *Angew. Chem., Int. Ed.* **2012**, *51*, 12810−12814.

(135) Choi, S.; Choi, K.-W.; Kim, S. K.; Chung, S.; Lee, S. *J. Phys. Chem. A* **2006**, *110*, 13183−13187.

(136) Jonsson, M.; Lind, J.; Merényi, G.; Eriksen, T. E. *J. Chem. Soc., Perkin Trans. 2* **1995**, 67−70.

(137) Bonifačić, M.; Asmus, K.-D. *J. Chem. Soc., Perkin Trans. 2* **1986**, 1805−1809.

(138) Zeng, H.; Sow, M.; Durocher, G. *J. Lumin.* **1994**, *62*, 1−16.

(139) Jacques, P.; Allonas, X.; Raumer, Von, M.; Suppan, P.; Haselbach, E. *J. Photochem. Photobiol., A* **1997**, *111*, 41−45.

(140) Ruiz, G.; Rodriguez-Nieto, F.; Wolcan, E.; Féliz, M. R. *J. Photochem. Photobiol., A* **1997**, *107*, 47−54.

(141) Singh, M. K.; Pal, H.; Sapre, A. V. *Photochem. Photobiol.* **2000**, *71*, 300−306.
(142) Weinberg, N. L.; Weinberg, H. R. *Chem. Rev.* **1968**, *68*, 449−523.
(143) Goto, Y.; Matsui, T.; Ozaki, S.-I.; Watanabe, Y.; Fukuzumi, S. *J. Am. Chem. Soc.* **1999**, *121*, 9497−9502.